

On the Feasibility of Electrode Concentration Distribution Estimation in Single-Particle Lithium-Ion Battery Models

Zahra Nozarijouybari^{ID}, Anirudh Allam^{ID}, Member, IEEE, Simona Onori^{ID}, Senior Member, IEEE, and Hosam K. Fathy^{ID}, Member, IEEE

Abstract—This letter analyzes the observability of a nonlinear single particle model (SPM) of a lithium-ion battery. SPMs offer an attractive middle ground between the simplicity of equivalent circuit models (ECMs) and the fidelity of higher-order electrochemical models. This can enable individual electrode concentration estimation via algorithms such as interconnected observers. Limitations exist on the feasibility and accuracy of such estimation, and can be examined using metrics such as nonlinear observability. This letter presents a set of conditions under which one can estimate the spatial distribution of concentrations in a nonlinear SPM. Specifically, we examine a nonlinear SPM where terminal voltage and its resistive component are measured independently. Butler-Volmer polarization potentials are assumed to be concentration-dependent. Under these assumptions, we show that electrode spatial concentration distributions can be estimated if the Jacobian of the voltage measurements with respect to surface concentrations is full rank. This condition applies for an arbitrary finite difference discretization of solid-phase diffusion dynamics. This letter demonstrates this insight numerically, for a model of a nickel-manganese-cobalt (NMC) battery.

Index Terms—Concentration estimation, lithium-ion batteries, nonlinear observability, single particle models.

I. INTRODUCTION

THIS letter examines the feasibility of estimating the spatial distribution of active species in a single particle model of a lithium-ion battery. Such estimation can support battery management system (BMS) applications by enabling

Manuscript received 16 September 2022; revised 22 November 2022; accepted 13 December 2022. Date of publication 22 December 2022; date of current version 6 January 2023. Support for this work was provided by the University of Maryland (through startup funding to H. K. Fathy) and Stanford University (through Precourt Energy Institute funding to S. Onori). Recommended by Senior Editor R. S. Smith. (*Corresponding author: Zahra Nozarijouybari.*)

Zahra Nozarijouybari and Hosam K. Fathy are with the Mechanical Engineering Department, University of Maryland, College Park, MD 20742 USA (e-mail: znozarij@umd.edu; hfathy@umd.edu).

Anirudh Allam and Simona Onori are with the Department of Energy Science and Engineering, Stanford University, Mountain View, CA 94305 USA (e-mail: aallam@stanford.edu; sonori@stanford.edu).

Digital Object Identifier 10.1109/LCSYS.2022.3231557

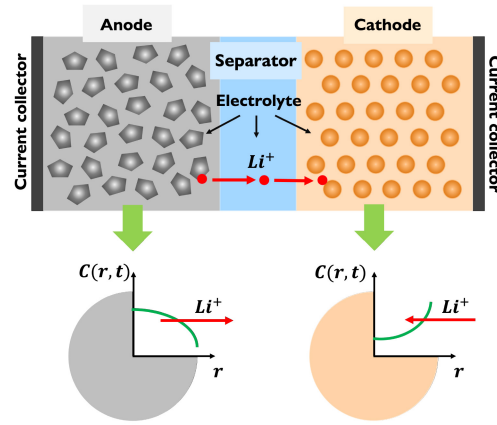


Fig. 1. Schematic representation of a single particle model.

individual electrode monitoring, battery chemistry characterization, and the tracking of aging/degradation [1]. Battery state estimation can be performed using either data-driven [2] or model-based approaches [3]. Two main types of models are often used for model-based estimation, namely: (i) equivalent circuit models and (ii) physics-based or electrochemical models. ECMs typically represent battery dynamics using series and parallel connections of (possibly nonlinear) resistors and capacitors. Their computational efficiency is appealing for BMS applications, but they can be difficult to fit to higher-order battery behaviors [4]. In contrast, electrochemical models, such as the Doyle-Fuller-Newman model [5], typically utilize fundamental physical laws to describe complex coupled phenomena such as diffusion, migration, precipitation, and oxidation/reduction [6]. However, their computational cost is often prohibitive for BMS applications. This motivates the pursuit of different strategies for battery model simplification [7], approximation [8], [9], [10], [11], reduction [12], [13], and/or reformulation [14]. The single particle model (Fig. 1) is one example of this pursuit. It models each electrode using a representative spherical particle while neglecting electrolytic diffusion. Its simplicity is appealing for BMS applications, one example being automotive battery state estimation at low

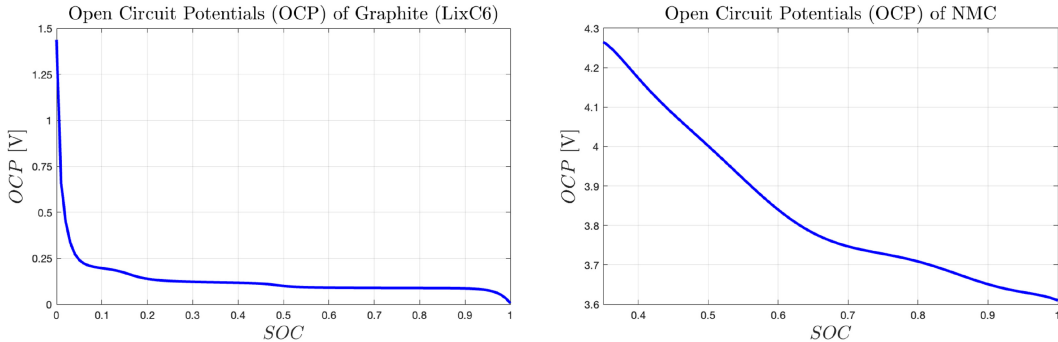


Fig. 2. Anode and cathode side open circuit potentials versus electrode states of charge.

charge/discharge C-rates. Moreover, the fact that SPMs model both anode- and cathode-side diffusion dynamics makes them useful for monitoring the dynamics of these electrodes independently. Examples of such independent monitoring include interconnected battery state observers [15], as well as virtual third reference electrodes [10]. SPM accuracy typically deteriorates at high charge/discharge rates because of failure to capture electrolyte dynamics [16]. To overcome this shortcoming, one can add electrolyte dynamics to obtain an enhanced single particle model (ESPM).

Regardless of the model used for estimation, limitations exist on estimation feasibility and accuracy. These limitations can be analyzed using different metrics, including linear and nonlinear observability. For instance, nonlinear observability analysis of an ECM by Zhao et al. [17] reveals that the first derivative of open circuit voltage (OCV) with respect to SOC is not the only factor affecting observability; higher derivatives also matter. Bartlett et al. [18] study nonlinear observability for an electrochemical model using Lie algebra. Moreover, Allam and Onori [15] investigate the effect of cathode material selection, battery cycling current magnitude, and battery model discretization on the observability of individual electrode concentrations. This work highlights the key differences between nonlinear and linear observability, including the fact that the input current trajectory affects observability. Li et al. [19] perform observability analysis for a physics-based fractional order model and assert that the similarity between the dynamics of the two electrodes, together with the large number of parameters to estimate, pushes the observability matrix close to singularity. Finally, Wu et al. [20] analyze an improved reduced-order model (iROM) for observability, and report that their proposed model reduction improves observability.

The goal of this letter is to examine nonlinear SPM observability assuming it is possible to independently measure overall battery voltage and the resistive component of this voltage, possibly through online impedance measurement. This letter assumes that a nonzero portion of the above voltages arises from Butler-Volmer reaction kinetics that are dependent on solid-phase surface ion concentrations. Under these assumptions, we show that the nonlinear SPM's electrode concentration distributions can be estimated, provided the Jacobian of the above two voltage measurements with respect to surface concentrations is full rank. This condition applies to an arbitrarily fine spatial discretization of the partial differential

equations (PDEs) governing solid-phase lithium concentrations. To the best of our knowledge, this condition is a novel and unique contribution to the literature. This letter demonstrates this condition through the numerical simulation of a commercial NMC battery model.

The remainder of this letter is organized as follows. Section II presents the SPM used in the letter's analyses. Section III presents the letter's conditions for estimation feasibility. Section IV demonstrates the letter's results in simulation. Finally, Section V summarizes the letter's conclusions.

II. SINGLE PARTICLE MODEL

This section presents the SPM used in this letter, building on previous work in the literature. Let $y(t)$ be the output voltage difference between the battery terminals at time t . This voltage depends on the input current, $u(t)$, as well as the anode- and cathode-side solid-phase lithium surface concentrations, x_a and x_c , respectively, as shown below:

$$y = -g_a(x_a) + g_c(x_c) - R_{total}u(t) - \eta_a(x_a) + \eta_c(x_c) \quad (1)$$

In this equation, R_{total} is the battery cell's Ohmic resistance. The functions g_a and g_c are the anode- and cathode-side equilibrium potentials, respectively, expressed in terms of the corresponding surface concentrations. Figure 2 plots g_a (obtained from [21]) and g_c (measured experimentally by the authors) versus the corresponding electrode states of charge. Moreover, the quantities η_a and η_c are the anode- and cathode-side reaction overpotentials.

The above equilibrium potentials and overpotentials both depend on solid-phase lithium surface concentrations. These concentrations are, in turn, governed by Fick's law of diffusion, as given in Eq. (2),

$$\frac{\partial C_{s,j}(r, t)}{\partial t} = \frac{D_{s,j}}{r^2} \frac{\partial}{\partial r} [r^2 \frac{\partial C_{s,j}(r, t)}{\partial r}] \quad (2)$$

where $D_{s,j}$ represents solid-phase diffusivity (assumed spatially constant) for either of the two active electrode materials; $C_{s,j}(r, t)$ is the solid phase concentration in each electrode as a function of radius r and time t ; and j refers to either a for the anode or c for the cathode. The quantities x_a and x_c in Eq. (1) can therefore be expressed as:

$$\begin{aligned} x_a(t) &= C_{s,a}(R_a, t) \\ x_c(t) &= C_{s,c}(R_c, t) \end{aligned} \quad (3)$$

These diffusion dynamics meet two boundary conditions:

$$\frac{\partial C_{s,j}}{\partial r}|_{r=0} = 0, \frac{\partial C_{s,j}}{\partial r}|_{r=R_j} = \frac{u}{Fa_{s,j}AL_jD_{s,j}} \quad (4)$$

where F is Faraday's constant, $a_{s,j}$ is the electrode specific interfacial surface area, A is the cell cross sectional area, L_j is the electrode thickness, and u is the battery input current (assumed positive during discharge). Finally, the Butler-Volmer equation represents the dependence of the anode- and cathode-side reaction overpotentials, η_a and η_c , respectively, on the applied current [6]:

$$u = \frac{Ai_0C_{s,j}}{C^*} \sinh\left(\frac{\alpha_j z F}{R_g T} \eta_j\right) \quad (5)$$

where i_0 is the exchange current density, C^* is a reference specific active material concentration [6], α_j is the charge transfer coefficient (set to 0.5 for this formulation), z is the number of electrons involved in the electrode reaction, R_g is the universal gas constant, T is the absolute temperature, and η_j is the electrode overpotential. Exchange current density, i_0 , is assumed constant for simplicity, but can be expressed as a function of species concentrations. Eq. (5) applies to both the anode and cathode, providing two overpotentials that collectively contribute to the overall battery cell overpotential.

The overpotentials on the anode and cathode sides can be embedded into the battery terminal voltage equation. The magnitudes of these overpotentials depend on several factors, including: (i) ionic conductivity of the electrolyte, and electronic conductivity of the electroactive materials and current collectors (namely Ohmic overpotential); (ii) the contact resistance between the current collector and the electroactive materials; (iii) the activation energy at the electrode surface (corresponding to the charge transfer overpotential); and (iv) lithium ion diffusion, especially near the electrode surface, and solid-state diffusion inside the electrode active material (corresponding to diffusion overpotential) [22].

The goal of this letter is to examine a set of conditions under which the above model's spatial concentration distributions can be feasibly estimated, assuming the input current $u(t)$ and output voltage $y(t)$ (including its resistive component) to both be measured. Mathematically, the focus of this letter is on a set of sufficient conditions for the local nonlinear structural observability of the above SPM.

III. NONLINEAR OBSERVABILITY ANALYSIS

To analyze observability, consider the charge transfer overpotential, η_j , in the Butler-Volmer Equation, Eq. (5). Solving for this overpotential gives:

$$\eta_j = \frac{R_g T}{\alpha_j z F} \sinh^{-1}\left(\frac{u C^*}{A i_0 C_{s,j}}\right) \quad (6)$$

The above equation can be simplified by defining the following lumped parameters: $\beta_j = R_g T / \alpha_j z F$, $\mu_j = A i_0 / C^*$. This makes it possible to define two battery output variables in Eq. (5): an instantaneous open-circuit potential $y_1(t)$ governed by the anode- and cathode-side surface concentrations, plus a

resistive overpotential, $y_2(t)$, that contains both Butler-Volmer and Ohmic overpotentials.

$$y(t) = y_1(t) + y_2(t)$$

$$\begin{aligned} y_1 &= g_c(x_c) - g_a(x_a) \\ y_2 &= \beta_c \sinh^{-1} \frac{u}{\mu_c x_c} - \beta_a \sinh^{-1} \frac{u}{\mu_a x_a} - R_{total} u \end{aligned} \quad (7)$$

The observability analysis in this letter builds on three insights. First, the voltage $y_2(t)$ represents a nonlinear resistive effect, and therefore depends on the instantaneous input current, $u(t)$. This leads to the key assumption that, in a battery equipped with online resistance measurement capabilities, it may be possible to measure the two output variables, $y_1(t)$ and $y_2(t)$, independently. Second, the resistive component of the overall battery output voltage, $y_2(t)$ includes surface concentration-dependent overpotential effects. This suggests that it may be possible to estimate surface concentrations from battery output measurements. Third, once surface concentrations are estimated for each electrode independently, it is possible to use the time derivatives of these concentrations to estimate the spatial distribution of charge in each electrode. Together, these three insights constitute the core foundations of this letter's analysis. The key ideas behind this analysis are that: (i) the two electrode surface concentrations can be estimated if the Jacobian of the output voltage measurements with respect to these concentrations is full rank; and (ii) once these electrode surface concentrations are known at every instant in time, Fick's law of diffusion can be used for inferring spatial concentration distributions. These ideas are outlined in the two results below.

Theorem 1: Consider the problem of solving Eq. (7) for $x_a(t)$ and $x_c(t)$, given measurements of $y_1(t)$ and $y_2(t)$ at time t . A solution of this problem, $x_a^*(t)$ and $x_c^*(t)$, is locally unique if the Jacobian of the outputs $y_1(t)$ and $y_2(t)$, evaluated at $x_a^*(t)$ and $x_c^*(t)$, is full rank.

To prove this theorem, suppose that $x_a^*(t)$ and $x_c^*(t)$ is a solution to Eq. (7) at time t . If the Jacobian of Eq. (7) at this solution is J , and if it is full rank, then the only solution to the equation $J[\delta x_a, \delta x_c]^T = \mathbf{0}$ is $[0, 0]^T$. Therefore, it will not be possible to perturb $x_a^*(t)$ and $x_c^*(t)$ by an infinitesimal amount while still solving Eq. (7).

Theorem 1 provides a sufficient condition for the unique local estimation of the anode- and cathode-side surface concentrations. This result is derived assuming a constant exchange current density, i_0 , but generalizes to the case where i_0 is a function of surface concentrations. Building on this result, the following lemma shows that once these surface concentrations are known versus time, differentiating them with respect to time enables the estimation of both the anode- and cathode-side spatial concentration distributions, for an arbitrary finite-difference discretization of Fick's law of diffusion.

Lemma 1: Consider an arbitrary finite-difference discretization of Fick's law, Eq. (2), for either the anode or cathode of a battery. Suppose that the input current, $u(t)$, is a known function of time. Moreover, suppose that the surface concentration, $x_a(t)$ or $x_c(t)$, is also a known function of time. Then

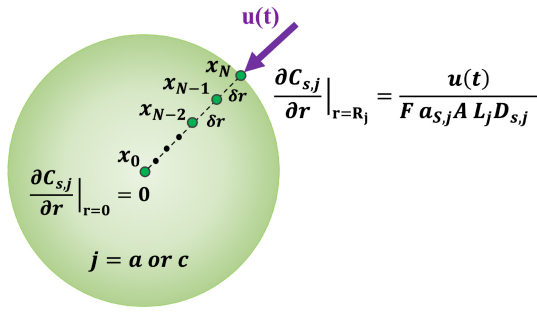


Fig. 3. Finite-difference discretization of Fick's law for a spherical diffusion medium.

TABLE I
BATTERY MODEL PARAMETERS

Parameter	Value	Unit
$D_{s,a}$	1.4493×10^{-14}	$m^2 s^{-1}$
$D_{s,c}$	5.8811×10^{-14}	$m^2 s^{-1}$
R_a	4.2642×10^{-6}	m
R_c	5.1592×10^{-7}	m
L_a	4.0000×10^{-5}	m
L_c	3.6550×10^{-5}	m
A	0.1048	m^2

the spatial distribution of concentration in the given electrode, $C_{s,j}$ can be uniquely computed at every instant in time.

The above lemma is validated by construction, as illustrated in Fig. 3. In this illustration, concentration is discretized in space to furnish a vector $[x_0(t), x_1(t), \dots, x_N(t)]^T$. Knowledge of surface concentration, which is achievable from the results of Theorem 1, automatically yields $x_N(t)$. Moreover, the boundary condition at $r = R_j$, together with knowledge of $u(t)$ and $x_N(t)$, makes it possible to compute $x_{N-1}(t)$. The time derivative of $x_{N-1}(t)$, together with Fick's law, then furnishes $x_{N-2}(t)$. The process can be repeated until all values of $x_i(t)$ are known, and can be extended to the more general case where diffusivity depends on species concentration.

Together, the above two results indicate that the spatial distribution of solid-phase concentrations in a lithium-ion battery model is locally structurally observable, provided the resistive and non-resistive components of terminal voltage can be measured independently and that their concentration dependence furnishes a full-rank Jacobian. The next section illustrates these results numerically, for an SPM of a commercial lithium-ion battery chemistry.

IV. NUMERICAL EXAMPLE

This section demonstrates the above insights using a lithium-ion battery SPM [23]. The simulated battery is a US18650VTC4 (Sony) type cell with an NMC cathode and graphite anode. The main specifications of the cell are: a 2Ah rated capacity, a 3.7V nominal voltage, and 4.2V/2.5V maximum/minimum voltage limits, respectively. The model's parameters are listed in Table I.

The above model is used in two demonstration studies, with each study focusing on one of the main results in this letter (namely, Theorem 1 and Lemma 1, respectively).

A. Demonstration Study #1: Surface Concentration Estimation

In this study, multiple constant-current charge/discharge profiles are simulated for the above SPM, starting from equilibrium at 0% SOC for the charge profiles and 100% SOC for the discharge profiles. The C-rates examined in these simulations are 0.5C, 1C, and 2C. The duration of the simulation is set to 1h(3600s) for the 0.5C and 1C currents, and 0.5h(1800s) for the 2C current. The simulation terminates either when its full time duration is reached or when a constraint is violated (e.g., minimum/maximum cell voltage limit, etc.). For each simulation, the SPM computes the battery terminal voltage, $y(t)$, the resistive component of this voltage, $y_2(t)$, and the non-resistive component of this voltage, $y_1(t) = y(t) - y_2(t)$. An optimization problem is then solved, at every time, t , to estimate $x_a(t)$ and $x_c(t)$ from $y_1(t)$ and $y_2(t)$. The optimization objective is given by:

$$\min_{x_a, x_c} (y_1 - y_{est,1})^2 + \gamma (y_2 - y_{est,2})^2 \quad (8)$$

where $y_{est,1}$ and $y_{est,2}$ are the estimated voltage components, optimization is performed subject to Eq. (7) as a constraint, and γ is a factor representing the relative importance of the accurate estimation of the two output voltages. Different choices of γ are possible. In this example, the value $\gamma = 1000$ is chosen for demonstration purposes. This is partly a reflection of the fact that, while the problems of estimating y_1 and y_2 are both important, the value of y_2 is typically much smaller than the value of y_1 .

The above estimation problem is solved at every time instant, with a 1-second sampling time, using a 100-point multi-start search employing the MATLAB function *fminsearch*. The outcome of this optimization is refined by replacing the solution furnished by multi-start *fminsearch* with the average of the estimates obtained for the preceding and following instants in time if this average furnishes a smaller objective function value. Finally, the outcomes of this comparison are passed through an 80-point moving average filter to produce the results in Fig. 4 for the 1C charge/discharge cases.

As evident from Fig. 4, the estimated surface concentration on both the anode and cathode side is in good agreement with the simulation results. Moreover, as shown in Tab. II, similarly attractive results are obtained at multiple C-rates, with good percentage root mean square surface concentration estimation errors (RMSE, normalized with respect to the corresponding electrodes' average concentration over the course of the simulation). This demonstrates the insight that when the Butler-Volmer polarization overpotentials depend on surface concentrations, it may indeed be possible to estimate the individual electrode surface concentrations from measurements of $y_1(t)$ and $y_2(t)$. Figure 5 plots the history of the reciprocal condition number of the Jacobian of $y_1(t)$ and $y_2(t)$, with respect to surface concentrations, estimated using the MATLAB function *rcond*, for the 1C charge case. Poor conditioning of this Jacobian, particularly around $t \approx 0.5h$, explains the corresponding inaccuracies in surface concentration estimation.

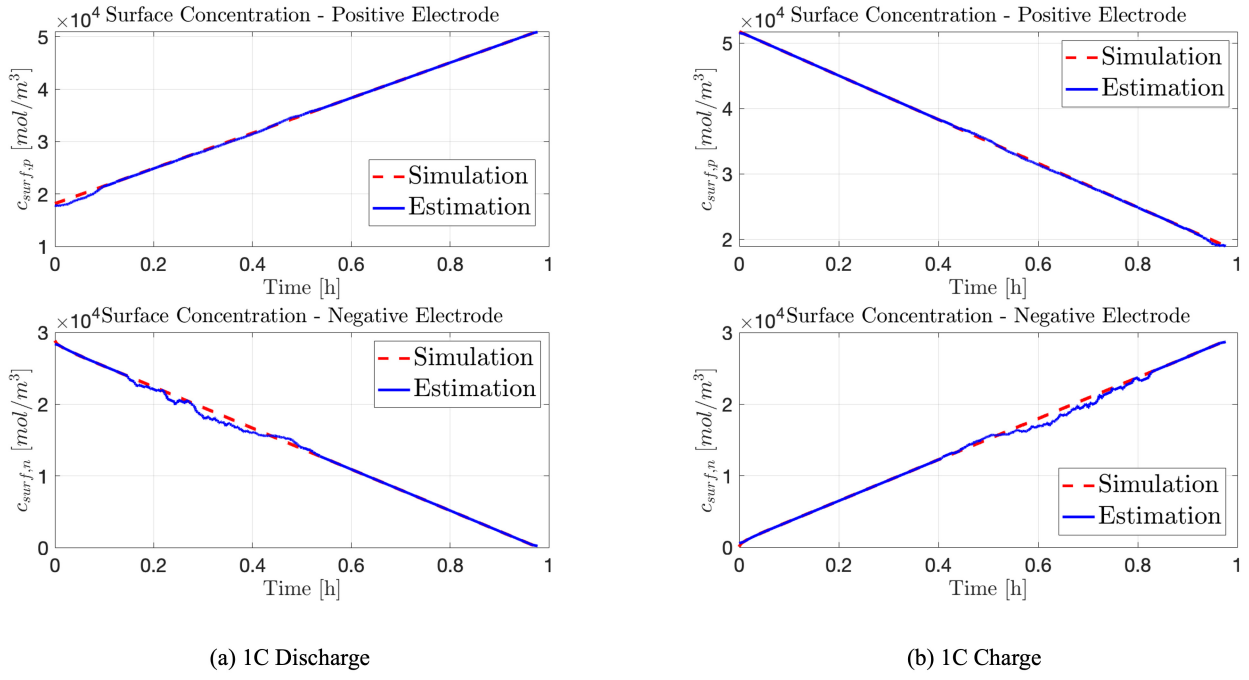


Fig. 4. Results of surface concentration estimation for the negative and positive electrodes.

TABLE II
RMS SURFACE CONCENTRATION ESTIMATION ERRORS

C-Rate	% RMSE (Anode)	% RMSE (Cathode)
2C Charge	8.35	2.07
1C Charge	9.0	1.63
0.5C Charge	7.88	2.48
0.5C Discharge	5.03	0.587
1C Discharge	9.58	1.08
2C Discharge	7.89	0.973

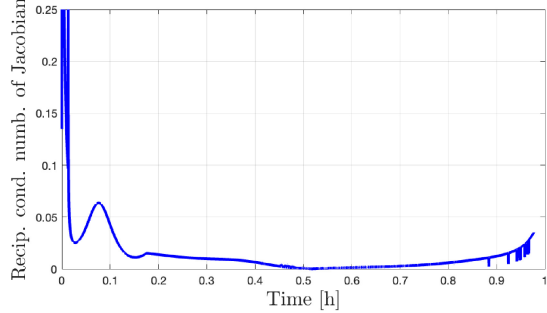


Fig. 5. Jacobian conditioning for surface conc. estimation.

B. Demonstration Study #2: Conc. Distribution Estimation

This study focuses on demonstrating the use of Fick's law for inferring electrode concentration distributions from surface concentration estimates. The study examines anode-side estimation for the 1C discharge case. We use finite differences to discretize Fick's law. We introduce some mismatch between the plant model and the observer by using 10 discretization points for the former versus 6 for the latter. One can, in theory, employ successive differentiation of surface concentration versus time for state estimation, following the

proof of Lemma #2. However, this will amplify noise in the surface concentration estimates. With this in mind, this study uses a Leunberger observer for estimating the spatial concentration distribution. Ackermann's formula is used for spacing the closed-loop observer poles linearly between $-0.1s^{-1}$ and $-0.4s^{-1}$. The observer is simulated with battery current $u(t)$ as its input and anode-side surface concentration as its output.

Figure 6 shows the results of the Leunberger estimation, with 80-point moving average filtering, for multiple locations in the anode, starting with zero initial conditions. The observer converges to a good estimate of concentration at all locations, demonstrating the fact that knowledge of surface concentration can be used for estimating spatial concentration distribution. These results are obtained using the surface concentration profile from the SPM, as opposed to the noisier profile from the surface concentration estimator. The use of the noisier surface concentration estimates in the Leunberger observer generates noisier but convergent estimates of spatial concentration distribution. This suggests that the ultimate implementation of this letter's insights should ideally employ a feedback estimation structure similar to the literature's interconnected observers.

V. SUMMARY AND CONCLUSION

This letter analyzes the nonlinear observability of a single particle lithium-ion battery model. This analysis furnishes sufficient conditions for observability of SPMs being that: (i) Butler-Volmer polarization potentials are functions of surface concentration, (ii) the resistive component of the terminal voltage be separately measured, and (iii) the Jacobian of the resistive and non-resistive components of the terminal voltage with respect to anode- and cathode-side surface concentrations be full-rank. With these conditions, regardless of the electrode spatial discretization, the SPM is locally structurally

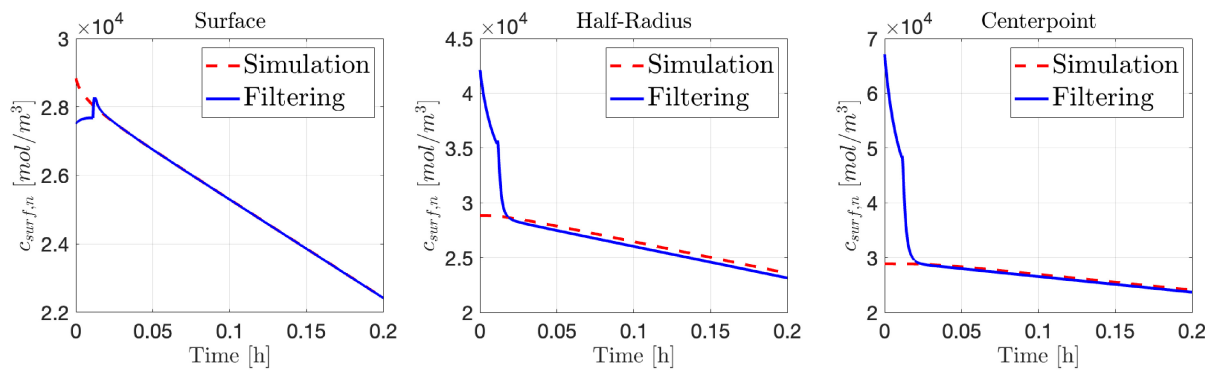


Fig. 6. Concentration estimation results at different spatial locations in the negative electrode.

observable. This condition is numerically demonstrated using an observer designed for separate electrode surface and spatial concentration distribution estimation, with the main goal of the work being to analyze fundamental limitations on battery state observability as opposed to proposing a new observer design. An experimentally-validated SPM for a commercial NMC cell is used in this letter and the results from the observer are compared to simulation. Potential future research directions include extending this letter's analysis to different chemistries, dynamic (as opposed to constant current) test profiles, different measurements (including stress/strain) [24], as well as models that are potentially more applicable to high C-rate scenarios (e.g., ESPMs that capture the dependence of overall battery resistance on electrolyte concentration, as well as temperature-dependent battery models).

REFERENCES

- [1] Y. Wang et al., "A comprehensive review of battery modeling and state estimation approaches for advanced battery management systems," *Renew. Sustain. Energy Rev.*, vol. 131, Oct. 2020, Art. no. 110015.
- [2] S. Li, H. He, C. Su, and P. Zhao, "Data driven battery modeling and management method with aging phenomenon considered," *Appl. Energy*, vol. 275, Oct. 2020, Art. no. 115340.
- [3] X. Hu, F. Feng, K. Liu, L. Zhang, J. Xie, and B. Liu, "State estimation for advanced battery management: Key challenges and future trends," *Renew. Sustain. Energy Rev.*, vol. 114, Oct. 2019, Art. no. 109334.
- [4] X. Hu, S. Li, and H. Peng, "A comparative study of equivalent circuit models for li-ion batteries," *J. Power Sources*, vol. 198, pp. 359–367, Jan. 2012.
- [5] M. Doyle, T. F. Fuller, and J. Newman, "Modeling of galvanostatic charge and discharge of the lithium/polymer/insertion cell," *J. Electrochem. Soc.*, vol. 140, no. 6, p. 1526, 1993.
- [6] A. J. Bard, L. R. Faulkner, and H. S. White, *Electrochemical Methods: Fundamentals and Applications*. Hoboken, NJ, USA: Wiley, 2022.
- [7] S. Santhanagopalan, Q. Guo, P. Ramadas, and R. E. White, "Review of models for predicting the cycling performance of lithium ion batteries," *J. Power Sources*, vol. 156, no. 2, pp. 620–628, 2006.
- [8] V. R. Subramanian, V. D. Diwakar, and D. Tapriyal, "Efficient macro-micro scale coupled modeling of batteries," *J. Electrochem. Soc.*, vol. 152, no. 10, 2005, Art. no. A2002.
- [9] C. Li, N. Cui, C. Wang, and C. Zhang, "Reduced-order electrochemical model for lithium-ion battery with domain decomposition and polynomial approximation methods," *Energy*, vol. 221, Apr. 2021, Art. no. 119662.
- [10] Z. Nozarijouybari and H. K. Fathy, "On the feasibility of developing virtual reference electrodes for lithium-ion batteries," in *Proc. Amer. Control Conf. (ACC)*, 2022, pp. 5247–5252.
- [11] D. Zhang, S. Park, L. D. Couto, V. Viswanathan, and S. J. Moura, "Beyond battery state of charge estimation: Observer for electrode-level state and cyclable lithium with electrolyte dynamics," *IEEE Trans. Transp. Electricif.*, early access, Jul. 14, 2022, doi: [10.1109/TTE.2022.3191136](https://doi.org/10.1109/TTE.2022.3191136).
- [12] V. S. Kumar, "Reduced order model for a lithium ion cell with uniform reaction rate approximation," *J. Power Sources*, vol. 222, pp. 426–441, Jan. 2013.
- [13] J. C. Forman, S. Bashash, J. L. Stein, and H. K. Fathy, "Reduction of an electrochemistry-based li-ion battery model via quasi-linearization and pade approximation," *J. Electrochem. Soc.*, vol. 158, no. 2, p. A93, 2010.
- [14] P. W. Northrop, B. Suthar, V. Ramadesigan, S. Santhanagopalan, R. D. Braatz, and V. R. Subramanian, "Efficient simulation and reformulation of lithium-ion battery models for enabling electric transportation," *J. Electrochem. Soc.*, vol. 161, no. 8, 2014, Art. no. E3149.
- [15] A. Allam and S. Onori, "Linearized versus nonlinear observability analysis for lithium-ion battery dynamics: Why respecting the nonlinearities is key for proper observer design," *IEEE Access*, vol. 9, pp. 163431–163440, 2021.
- [16] X. Han, M. Ouyang, L. Lu, and J. Li, "Simplification of physics-based electrochemical model for lithium ion battery on electric vehicle. Part I: Diffusion simplification and single particle model," *J. Power Sources*, vol. 278, pp. 802–813, Mar. 2015.
- [17] S. Zhao, S. R. Duncan, and D. A. Howey, "Observability analysis and state estimation of lithium-ion batteries in the presence of sensor biases," *IEEE Trans. Control Syst. Technol.*, vol. 25, no. 1, pp. 326–333, Jan. 2017.
- [18] A. Bartlett, J. Marcicki, S. Onori, G. Rizzoni, X. G. Yang, and T. Miller, "Electrochemical model-based state of charge and capacity estimation for a composite electrode lithium-ion battery," *IEEE Trans. Control Syst. Technol.*, vol. 24, no. 2, pp. 384–399, Mar. 2016.
- [19] X. Li et al., "A physics-based fractional order model and state of energy estimation for lithium ion batteries. Part I: Model development and observability analysis," *J. Power Sources*, vol. 367, pp. 187–201, Nov. 2017.
- [20] L. Wu, K. Liu, and H. Pang, "Evaluation and observability analysis of an improved reduced-order electrochemical model for lithium-ion battery," *Electrochimica Acta*, vol. 368, Feb. 2021, Art. no. 137604.
- [21] Y. Ji, Y. Zhang, and C.-Y. Wang, "Li-ion cell operation at low temperatures," *J. Electrochem. Soc.*, vol. 160, no. 4, p. A636, 2013.
- [22] S. Ernst, T. P. Heins, N. Schlüter, and U. Schröder, "Capturing the current-overpotential nonlinearity of lithium-ion batteries by nonlinear electrochemical impedance spectroscopy (NLEIS) in charge and discharge direction," *Front. Energy Res.*, vol. 7, p. 151, Dec. 2019.
- [23] A. Allam and S. Onori, "An interconnected observer for concurrent estimation of bulk and surface concentration in the cathode and anode of a lithium-ion battery," *IEEE Trans. Ind. Electron.*, vol. 65, no. 9, pp. 7311–7321, Sep. 2018.
- [24] S. Pannala, P. Valecha, P. Mohtat, J. B. Siegel, and A. G. Stefanopoulou, "Electrochemical battery state estimation under parameter uncertainty caused by aging using expansion measurements," in *Proc. Amer. Control Conf. (ACC)*, 2021, pp. 3088–3093.